Ashish S. Kanthale, **International Journal of Research Welfare Society**
Volume 2, Issue 1, 2026, pp. 18-33
https://www.ijrws.com
ISSN: 3142-8657

RESEARCH ARTICLE OPEN ACCESS

Therapeutic Evaluation of Hedychium Spicatum in Smoking Induced COPD in Mice

Ashish S. Kanthale*, Vivek V. Paithankar,Anjali Wankhade, Jugal Vyas
Vidyabharati College of Pharmacy, Amravati,Maharashtra, India.

ABSTRACT: Chronic Obstructive Pulmonary Disease (COPD), the third leading cause of global mortality, lacks treatments that reverse disease progression. This study evaluated the hydroethanolic extract of Hedychium spicatum rhizomes (HEE-HS), administered via nebulisation, in a cigarette smoke-induced COPD mouse model, compared against the standard drug roflumilast.

Thirty Swiss albino mice were divided into five groups: normal control, disease control, roflumilast (1 mg/kg oral), and HEE-HS at 100 and 200 mg/kg nebulised over 35 days. GC-MS analysis identified 1,8-cineole (28.6%), camphor (15.3%), and β-caryophyllene (12.8%) as dominant bioactive constituents, with an established LD_{50} >2000 mg/kg.

HEE-HS at 200 mg/kg significantly reversed all COPD-related parameters, including body weight loss, lung hypertrophy, airflow obstruction ($FEV_{0.1}$/FVC improved by 43.6%), neutrophilic inflammation in bronchoalveolar lavage fluid, and elevated pro-inflammatory cytokines TNF-α and IL-6. Results were statistically comparable to roflumilast. Histopathology confirmed near-normal alveolar architecture with minimal collagen deposition.

These findings offer the first robust preclinical evidence supporting the traditional Ayurvedic use of H. spicatum in respiratory disease, advocating further mechanistic research and clinical translation.

Keywords: COPD; Hedychium spicatum; 1,8-cineole; cigarette smoke; nebulisation; roflumilast; BALF; TNF-α; IL-6; Zingiberaceae.

Date of acceptance:01-06-2026 Date of Publish: 30-06-2026

I. INTRODUCTION

1.1. Global burden and clinical significance of COPD

Chronic Obstructive Pulmonary Disease (COPD) is a common, preventable, and treatable chronic inflammatory lung disease characterised by persistent airflow limitation due to airway and alveolar abnormalities caused by significant exposure to noxious particles or gases [1,2]. It encompasses chronic bronchitis — clinically defined as chronic cough and sputum production for at least three months in two consecutive years — and emphysema, characterised anatomically by permanent destructive enlargement of airspaces distal to the terminal bronchioles [3]. COPD ranks as the third leading cause of mortality globally, accounting for over 3.23 million deaths in 2019 (WHO) [4]. The annual economic burden exceeds $49 billion in the United States alone [5]. In India, approximately 14.84 million individuals are affected; chronic bronchitis predominates owing to widespread biomass fuel combustion, tobacco chewing, and bidi smoking [6,7]. An estimated 95% of COPD cases are attributable to cigarette smoking [8].

1.2. Pathophysiology

COPD pathophysiology involves four converging axes.

(i) Oxidative stress: cigarette smoke introduces ROS ($O_2^{\bullet -}$, H_2O_2, •OH) directly and via activated inflammatory cells, overwhelming antioxidant defences (SOD, glutathione peroxidase, thioredoxin). Lipid peroxidation products — malondialdehyde (MDA) and 4-hydroxynonenal (4-HNE) — activate NF-κB/AP-1 signalling cascades [9,10].

(ii) Chronic airway inflammation: TLR and NLRP3 inflammasome activation drives neutrophil and macrophage recruitment; neutrophils release serine proteases and MMPs, while alveolar macrophages secrete MMP-9, MMP-12, TNF-α, IL-8, and LTB4 [11,12]. $CD8^+$ T-lymphocytes induce alveolar epithelial apoptosis via perforin and granzyme B, perpetuating emphysema [13].

(iii) Protease-antiprotease imbalance: excess neutrophil elastase over AAT, SLPI, and TIMPs

destroys alveolar walls and eliminates elastic recoil [14].
(iv) Mucus hypersecretion: goblet cell hyperplasia and MUC5AC/MUC5B upregulation impair mucociliary transport, promoting bacterial colonisation and exacerbations [15,16].

1.3. Limitations of current pharmacotherapy and rationale for herbal therapy Current COPD management relies on short- and long-acting bronchodilators (β2-agonists, anticholinergics), inhaled corticosteroids (ICS), and the PDE-4 inhibitor roflumilast. While these agents alleviate symptoms and reduce exacerbation frequency, none significantly modifies disease progression or reverses structural lung destruction [17]. Long-term corticosteroid use is associated with osteoporosis, diabetes mellitus, and increased infection susceptibility [18]. These limitations have generated growing interest in herbal and natural product-based therapeutics. Traditional medicine systems — Ayurveda, Traditional Chinese Medicine — document numerous plant-derived formulations used for centuries to manage respiratory ailments, with potential multi-target benefits by simultaneously modulating inflammation, oxidative stress, and mucociliary function, often with superior tolerability [19].

1.4. Hedychium spicatum: scientific rationale for selection

Hedychium spicatum Buch. Ham. (Zingiberaceae) — Ayurvedic name Shati or Kapur Kachari — is a perennial rhizomatous herb native to the Western and Central Himalayas (3,500–7,500 ft altitude), described in classical texts including Charaka Samhita and Sushruta Samhita as a remedy for Shwasa (dyspnoea), Kasa (cough), and pulmonary eosinophilia [20]. Phytochemical investigations identified 1,8-cineole, β-caryophyllene, camphor, linalool, borneol, hedychenone, and labdane diterpenes — bioactive compounds with documented bronchodilatory, anti-inflammatory, and antioxidant properties [21,22]. Worth et al. [23] demonstrated in a double-blind placebo-controlled randomised clinical trial that 1,8-cineole (200 mg three times daily) — a dominant constituent of H. spicatum essential oil — significantly improved FEV_1 by 9.5% and reduced exacerbations in COPD patients over 6 months. Juergens et al. [24] confirmed that 1,8-cineole potently inhibits TNF-α, IL-1β, and IL-6 in human monocytes via a dual anti-inflammatory mechanism analogous to corticosteroids, without adverse effects. Despite this compelling rationale, no systematic preclinical evaluation of H. spicatum in a validated COPD model existed prior to this study — a critical gap that the present investigation addresses.

1.5. Drug delivery by nebulisation

Inhalation is the gold standard for delivering drugs directly to the respiratory tract in COPD. Advantages include: targeted pulmonary delivery minimising systemic side effects; rapid onset of action; avoidance of first-pass hepatic metabolism; and high local drug concentrations at the site of inflammation [25]. Jet nebulisation generates aerosol droplets with mass median aerodynamic diameter (MMAD) 2–5 µm, enabling lower-airway and alveolar deposition [26]. For volatile, lipophilic, terpene-rich essential oils — such as HEE-HS — nebulisation maximises pulmonary bioavailability and directly targets airway inflammation, closely replicating traditional aromatherapeutic inhalation while enabling precise dosimetric control [27,28].

II. MATERIALS AND METHODS

2.1. Ethics

All animal experiments were performed in strict compliance with CPCSEA guidelines under prior IAEC approval, Vidyabharati College of Pharmacy, Amravati (Approval No. VBCP/IAEC/2025/03). Animals exhibiting signs of illness during acclimatisation were excluded. Humane endpoints and welfare standards were maintained throughout.

2.2. Plant material, extraction, and standardization

Fig. I : Hedychium Spicatum

Hedychium spicatum Buch. Ham. rhizomes were procured from high-altitude Western Himalayan forests during the peak harvest

season (October–November) and authenticated by Mrs. Lubna P. Khalid, Dept. of Botany, Vidyabharati Mahavidyalaya, Amravati. Dried rhizome powder was subjected to hydro-distillation for 4 hours using a Clevenger-type apparatus (IS: 3551) to obtain the hydroethanolic essential oil extract (HEE-HS). Extract yield: 2.38% w/w (dry weight basis). The extract was dried over anhydrous Na_2SO_4, filtered through Whatman No. 1 filter paper, and stored in sealed amber vials at 4°C under nitrogen atmosphere until use. Qualitative phytochemical screening followed Trease and Evans (2002) standard methods. GC-MS analysis determined quantitative chemical composition. Physico-chemical standardisation was performed per Table 1.

Table 1. Physico-chemical standardisation parameters of HEE-HS.

Parameter	**Standard / Specification**	**Observed Result**
Description	Light brownish-yellow powder	Complies
Odour	Camphoraceous-sweet, characteristic	Characteristic
Moisture content (% w/w)	6.82 ± 0.35	6.90
Ash content (% w/w)	7.14 ± 0.28	7.21
Acid-insoluble extract (% w/w)	1.08 ± 0.12	1.01
Water-soluble extractive (% w/w)	18.54 ± 0.52	18.80
Swelling index (mL/g)	2.8 ± 0.2	2.32
pH (1% aqueous solution)	6.2 ± 0.1	6.01
Particle size	≥80% through 63-mesh sieve	Complies

2.3. Chemicals and reagents

Roflumilast (pharmaceutical grade; MW 403.21 g/mol; Glenmark Pharmaceuticals, India) was the standard drug. Research-grade 3R4F cigarettes (University of Kentucky, USA; TPM: 9.4 mg/cig; nicotine: 0.73 mg/cig; CO: 12 mg/cig) were used for standardised smoke generation. All chemicals were analytical grade (Sigma-Aldrich USA; Merck Life Science India; HiMedia Laboratories India; S.D. Fine Chem India). Validated sandwich ELISA kits were used for TNF-α and IL-6 quantification. Histological stains: Harris's haematoxylin, eosin Y (HiMedia), and Masson's Trichrome kit (Sigma Aldrich).

2.4. Drug preparation and administration

HEE-HS was dissolved in 0.25% polysorbate-80 (Tween-80) in 0.9% NaCl to prepare a homogeneous emulsion freshly before each session; filtered through 0.22 µm sterile membrane filter before loading into nebuliser. An Omron nebuliser connected to the whole-body inhalation chamber delivered HEE-HS (30 min/session, once daily, commencing 30 min after the second CS exposure). Roflumilast was suspended in 0.5% CMC-Na/normal saline by probe sonication (30 s, 40 kHz) and administered by oral gavage once daily.

2.5. Experimental animals

Healthy adult Swiss albino mice (Mus musculus; outbred; 25–30 g; either sex) were procured from National Institute of Biosciences, Pune. Housing: groups of 3/cage (43 × 27 × 15 cm polypropylene; sterile paddy husk bedding changed every 48 h) at 23 ± 2°C, 55 ± 5% relative humidity, 12-h light/dark cycle (lights on 07:00 h), 15–20 air changes/hour, noise below 85 dB, standard rodent pellet diet and purified water ad libitum. Acclimatisation: 7 days before commencement.

2.6. Acute toxicity study

Acute oral toxicity of HEE-HS was determined per OECD Test Guideline 423 (limit dose: 2000 mg/kg). Animals were observed for 14 days for clinical signs, behavioural changes, and mortality. No mortality or significant adverse signs were observed; LD_{50} was established as > 2000 mg/kg, confirming a wide therapeutic window suitable for chronic dosing.

2.7. Experimental design and COPD induction

A randomised, parallel-group, controlled design was employed. Thirty mice were allocated by block randomisation into five groups (n = 6). CS exposure was conducted in a 30-litre whole-body inhalation chamber (5 cigarettes/session, 30 min/session, twice daily, 6 days/week, 35 consecutive days). Group I received filtered room air under identical schedules. Treatments were administered concurrently for the final 15 days (Table 2).

Table 2. Experimental group design (n = 6 per group).

Grp I	Group Name	COPD Induction	Treatment (Days 1–35)	Route
	Normal Control (NC)	Room air (filtered)	0.9% NaCl — nebulised vehicle	Inhalation
II	Disease Control (DC)	CS: 5 cig/session ×2 daily, 35 days	Vehicle only (nebulised)	Inhalation
III	Roflumilast — Standard	CS exposure	Roflumilast 1 mg/kg/day in 0.5% CMC-Na	Oral (p.o.)
IV	HEE-HS 100 mg/kg	CS exposure	HEE-HS 100 mg/kg/day (nebulised)	Inhalation
V	HEE-HS 200 mg/kg	CS exposure	HEE-HS 200 mg/kg/day (nebulised)	Inhalation

2.8. Outcome measures and statistical analysis

• Body weight: recorded weekly (Weeks 1–5). Lung weight and lung index (lung wt/body wt × 100) at sacrifice (Day 36) after cervical dislocation under 2–3% chloroform anaesthesia. • Pulmonary function: $FEV_{0.1}$/FVC ratio by Haward apparatus rodent spirometer on Day 36 prior to sacrifice.

• BALF: tracheal cannulation; 3 × 0.5 mL ice-cold PBS (pH 7.4) instilled; centrifuged at 400 × g, 10 min, 4°C. Total cell count by haemocytometer; differential count on Giemsa-stained cytospin slides (≥300 cells/slide counted).

• Cytokines: TNF-α and IL-6 in lung homogenate by validated sandwich ELISA (triplicates; protein-normalised as pg/mg protein). Right lung lobes snap-frozen in liquid nitrogen at −80°C. • Histopathology: left lobe inflation-fixed in 10% NBF (25 cm H_2O, 24 h); 4 µm paraffin sections stained with H&E and Masson's Trichrome (MT); photomicrographs at 100× and 400× magnification.

Statistics: one-way ANOVA followed by Tukey's multiple comparison post-hoc test (GraphPad Prism 9). Data expressed as mean ± SEM. Significance: *$p < 0.05$; **$p < 0.01$; ***$p < 0.001$.

III. RESULTS

3.1. Phytochemical screening and GC-MS characterisation

Preliminary phytochemical screening of HEE-HS confirmed the presence of alkaloids, saponins, carbohydrates, glycosides, flavonoids, reducing sugars, and tannins (Table 3). GC-MS profiling of the essential oil fraction identified 1,8-cineole as the dominant constituent (28.6%), followed by camphor (15.3%) and β-caryophyllene (12.8%), with minor contributions from linalool, borneol, α-pinene, and the furanoid diterpene hedychenone — a constituent unique to this species. All physicochemical standardisation parameters (Table 1) complied with pharmacopoeial specifications.

Table 3. Qualitative phytochemical screening of HEE-HS.

No. 1	Constituent	Test(s) Performed	Result
	Alkaloids	Dragendorff's test (orange-red ppt); Mayer's test (yellowish-white ppt)	+
2	**Saponins**	Foam test — stable foam on shaking for 15 min	+
3	**Carbohydrates**	Molisch's test (red-violet ring); Barfoed's test (red precipitate)	+
4	**Glycosides**	Killer-Killiani test (deep blue at junction); Legal test (pink colour in pyridine)	+
5	**Flavonoids**	Shinoda's reaction — yellow/red colour with Mg powder + conc. HCl	+
6	**Reducing Sugars**	Fehling's test — brick-red precipitate on heating	+
7	**Tannins**	$FeCl_3$ (green-black); Gelatin test (white ppt); Lead acetate (red ppt)	+
8	**Terpenoids**	Salkowski's test — 5ml extract + 2 ml chloroform + 3ml conc. H_2So_4 (Reddish brown colour at the interface)	+

[+ = present; − = absent]

3.2. Effect on body weight

CS exposure for 5 weeks caused a progressive and significant ($p < 0.001$) reduction in body weight in DC mice compared with NC (Week 5: DC 18.6 ± 0.24 g vs. NC 29.8 ± 0.37 g), reflecting catabolic sequelae of chronic pulmonary inflammation and systemic oxidative stress [8,9]. HEE-HS produced dose-dependent attenuation of body-weight loss (Table 4). At 200 mg/kg, Week-5 body weight (28.3 ± 0.24 g) was virtually identical to roflumilast (29.3 ± 0.29 g), indicating effective suppression of systemic inflammatory burden.

Table 4. Effect of CS exposure and HEE-HS treatment on body weight (g; mean ± SEM, n = 6).

Group	**Week 1**	**Week 2**	**Week 3**	**Week 4**	**Week 5**
I – Normal Control	28.2 ± 0.12	29.4 ± 0.21	28.4 ± 0.31	30.1 ± 0.41	29.8 ± 0.37
II – Disease Control	22.0 ± 0.14	21.2 ± 0.18	20.4 ± 0.33	19.5 ± 0.34	18.6 ± 0.24
III – Roflumilast 1 mg/kg	23.0 ± 0.16	24.1 ± 0.24	26.2 ± 0.40	28.4 ± 0.28	29.3 ± 0.29
IV – HEE-HS 100 mg/kg	22.4 ± 0.12	23.5 ± 0.16	24.1 ± 0.18	25.3 ± 0.28	26.4 ± 0.31
V – HEE-HS 200 mg/kg	21.3 ± 0.15	22.6 ± 0.21	23.9 ± 0.21	26.9 ± 0.32	28.3 ± 0.24

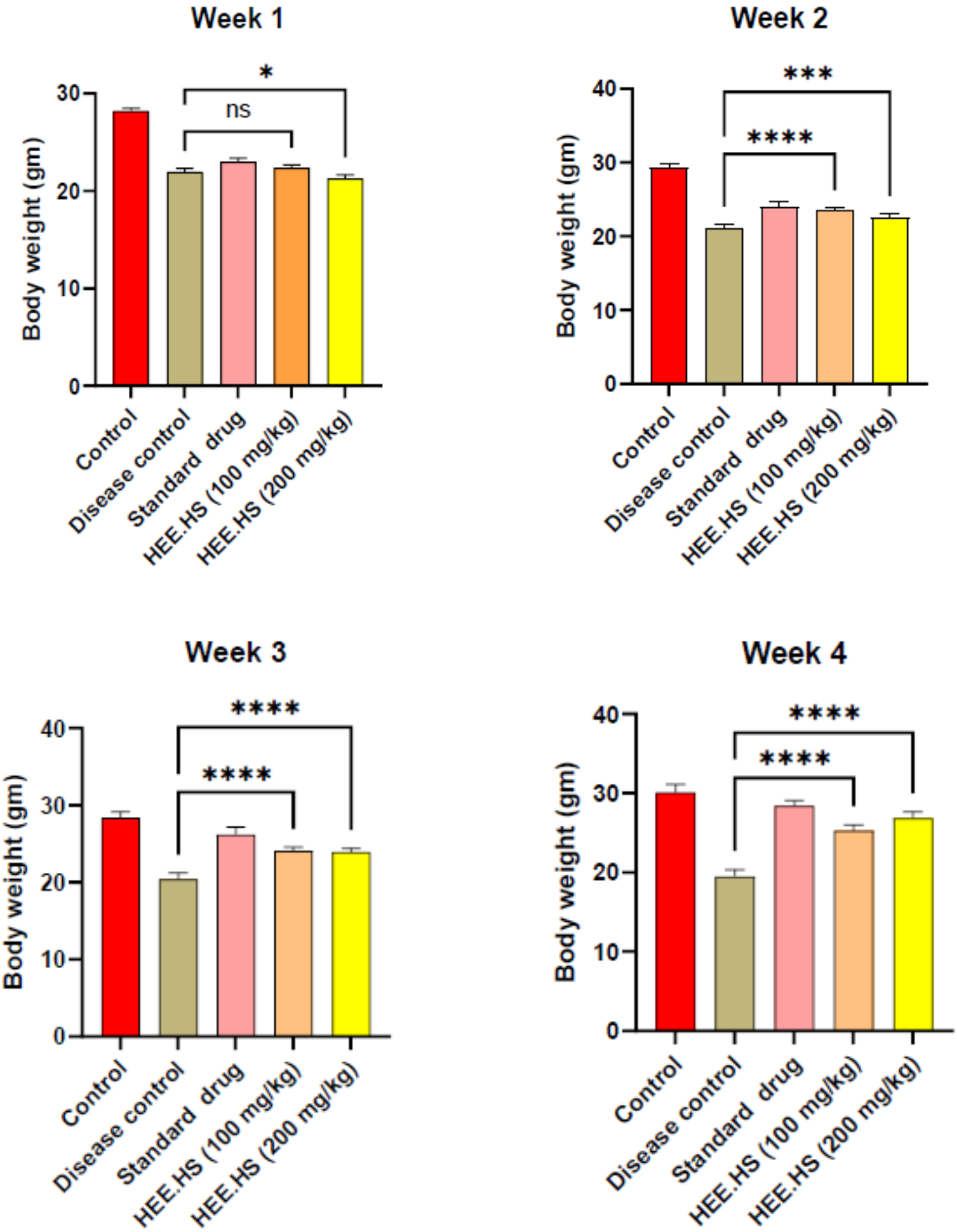
Week 1
Body weight (gm)
30
20
10
0
*
ns
Control
Disease control
Standard drug
HEE.HS (100 mg/kg)
HEE.HS (200 mg/kg)
Week 2
Body weight (gm)
40
30
20
10
0
***
****
Control
Disease control
Standard drug
HEE.HS (100 mg/kg)
HEE.HS (200 mg/kg)
Week 3
Body weight (gm)
40
30
20
10
0
****
****
Control
Disease control
Standard drug
HEE.HS (100 mg/kg)
HEE.HS (200 mg/kg)
Week 4
Body weight (gm)
40
30
20
10
0
****
****
Control
Disease control
Standard drug
HEE.HS (100 mg/kg)
HEE.HS (200 mg/kg)

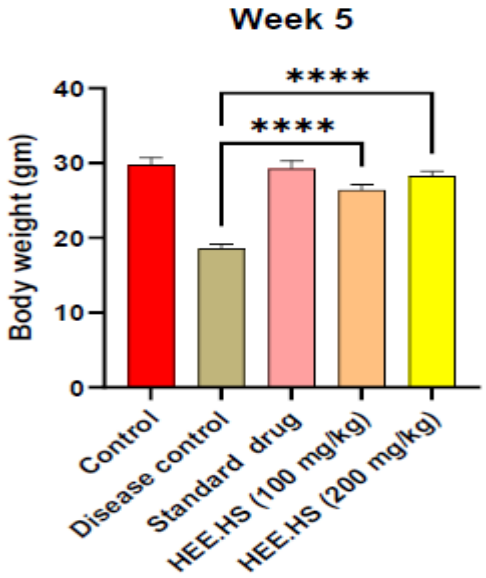

Fig 2. Effect of Cigarette Smoke Exposure on body weight

All values are expressed as mean ± SEM (n=6). Stastistical comparisions between each treatment and COPD induced mice were carried out by one way ANOVA followed by Turkey multiple comparisons test. ****p < 0.0001 when compared with COPD induced mice.

3.3. Lung weight and lung index

CS exposure significantly increased lung weight (DC: 0.2902 ± 0.0018 g vs. NC: 0.1485 ± 0.0008 g; $p < 0.001$) and lung index (DC: 1.170 ± 0.018 vs. NC: 0.519 ± 0.009; $p < 0.001$), reflecting severe pulmonary inflammation, oedema, and structural hypertrophy (Table 5). HEE-HS dose-dependently and significantly reduced both parameters. At 200 mg/kg, lung weight (0.2143 ± 0.0012 g) and lung index (0.800 ± 0.011) closely approached roflumilast values (0.2020 ± 0.0012 g; 0.745 ± 0.012), indicating effective attenuation of CS-induced pulmonary congestion.

Table 5. Effect on lung weight and lung index (mean ± SEM, n = 6).

Group I – Normal Control	**Lung Weight (g)**	**Lung Index**
	0.1485 ± 0.0008	0.519 ± 0.009
II – Disease Control	0.2902 ± 0.0018***	1.170 ± 0.018***
III – Roflumilast 1 mg/kg	0.2020 ± 0.0012	0.745 ± 0.012
IV – HEE-HS 100 mg/kg	0.2287 ± 0.0013	0.873 ± 0.014
V – HEE-HS 200 mg/kg	0.2143 ± 0.0012	0.800 ± 0.011

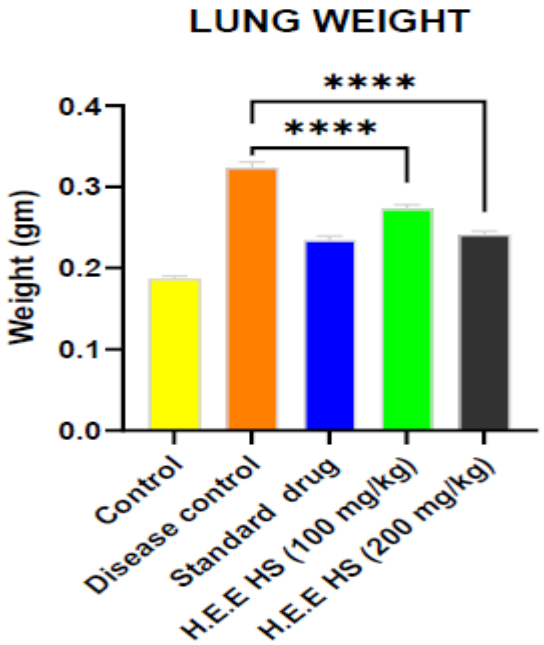

Fig 3 . Effect Of Cigarette Smoke Exposure on Lung Weight and Lung Index

All values are expressed as mean ± SEM (n=6). Stastistical comparisions between each treatment and COPD induced mice were carried out by one way ANOVA followed by Turkey multiple comparisions test. ****p < 0.0001 when compared with COPD induced mice.

3.4. Pulmonary function — $FEV_{0\cdot1}$/FVC ratio

CS exposure markedly reduced $FEV_{0\cdot1}$/FVC ratio in DC mice (54.3 ± 0.9% vs. 88.7 ± 1.2% in NC; $p < 0.001$), confirming obstructive airflow limitation characteristic of COPD (Table 6). HEE-HS produced dose-dependent, significant restoration. At 200 mg/kg, $FEV_{0\cdot1}$/FVC reached 78.0 ± 1.0% — a 43.6% improvement over DC — statistically indistinguishable from roflumilast (78.1 ± 1.1%; $p < 0.001$ vs. DC). The 100 mg/kg dose produced an intermediate improvement (69.4 ± 1.1%; +27.8% vs. DC). All treatment groups showed significant improvement vs. DC ($p < 0.001$).

Table 6. Pulmonary function: $FEV_{0\cdot1}$/FVC ratio (mean ± SEM, n = 6).

Group I – Normal Control	**$FEV_{0\cdot1}$ (mL)**	**FVC (mL)**	**$FEV_{0\cdot1}$/FVC (%)**	**% Improvement vs. DC**
	0.212 ± 0.003	0.239 ± 0.002	88.7 ± 1.2	—
II – Disease Control	0.138 ± 0.002	0.254 ± 0.003	54.3 ± 0.9***	—
III – Roflumilast 1 mg/kg	0.196 ± 0.002	0.251 ± 0.002	78.1 ± 1.1	+43.8%
IV – HEE-HS 100 mg/kg	0.172 ± 0.003	0.248 ± 0.002	69.4 ± 1.1	+27.8%
V – HEE-HS 200 mg/kg	0.192 ± 0.002	0.246 ± 0.002	78.0 ± 1.0	+43.6%

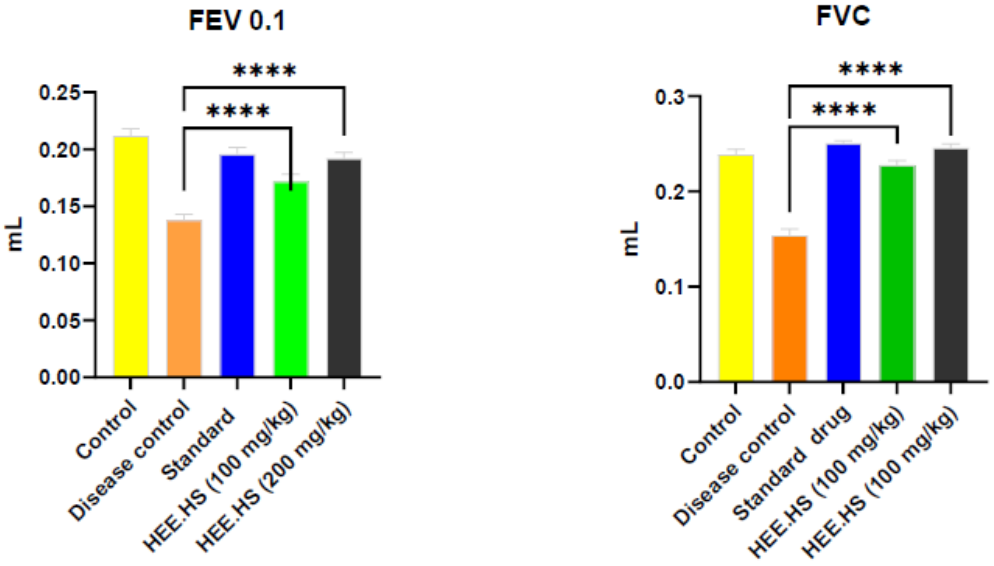

Fig 4 . Effect of Cigarette Smoke Exposure on Lung Function

3.5. BALF cellular composition

CS exposure caused approximately 9-fold elevation in total BALF cells (DC: $5.76 \pm 0.09 \times 10^5$/mL vs. NC: 0.64 ± 0.02; $p < 0.001$), accompanied by marked neutrophilia (DC: $28.33 \pm 0.67\%$ vs. NC: $3.80 \pm 0.15\%$) and a proportionate decline in macrophage dominance (DC: $58.50 \pm 0.76\%$ vs. NC: $92.42 \pm 0.45\%$; Table 7). HEE-HS 200 mg/kg significantly reduced total cells ($2.18 \pm 0.05 \times 10^5$/mL), neutrophil proportion ($13.17 \pm 0.31\%$), and lymphocyte count ($6.80 \pm 0.31\%$), approaching roflumilast values across all parameters ($p < 0.001$ vs. DC).

Table 7. BALF cellular composition (mean ± SEM, n = 6).

Group	**Total Cells (×10⁵/mL)**	**Macrophages (%)**	**Neutrophils (%)**	**Lymphocytes (%)**	**Eosinophils (%)**
I – Normal Control	0.64 ± 0.02	92.42 ± 0.45	3.80 ± 0.15	3.24 ± 0.12	0.60 ± 0.06
II – Disease Control	5.76 ± 0.09***	58.50 ± 0.76***	28.33 ± 0.67***	10.20 ± 0.30***	2.80 ± 0.19***
III – Roflumilast	1.94 ± 0.05	81.17 ± 0.60	10.50 ± 0.43	6.80 ± 0.20	1.40 ± 0.12
IV – HEE-HS 100 mg/kg	3.42 ± 0.07	70.83 ± 0.48	18.33 ± 0.33	8.60 ± 0.27	2.20 ± 0.12
V – HEE-HS 200 mg/kg	2.18 ± 0.05	78.67 ± 0.42	13.17 ± 0.31	6.80 ± 0.31	1.40 ± 0.10

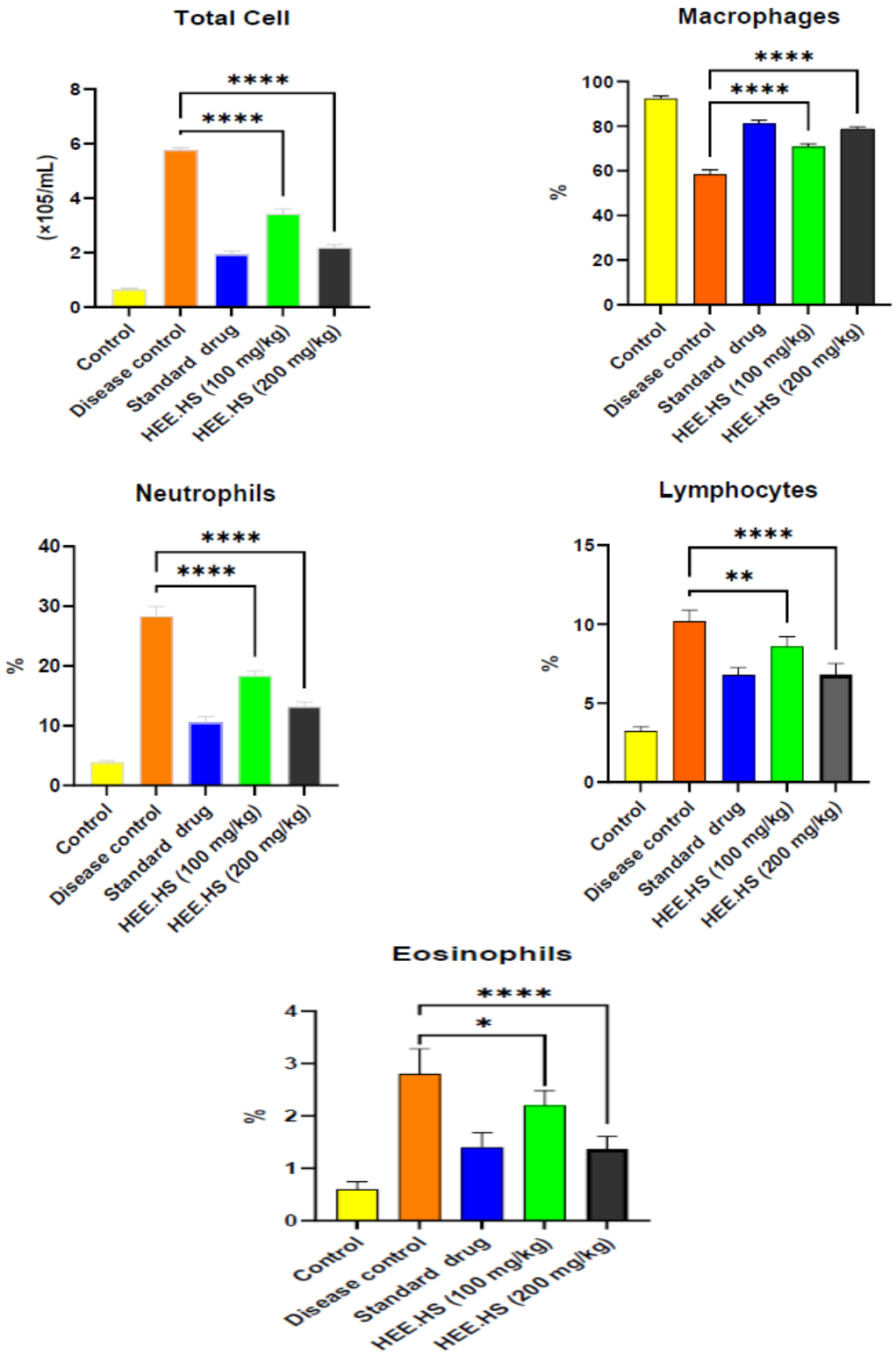

Fig 5. Effect of Cigarette Smoke Exposure on BALF Cellular Composition

All values are expressed as mean ± SEM (n=6). Stastistical comparisions between each treatment and COPD induced mice were carried out by one way ANOVA followed by Turkey multiple comparisions test. ****p < 0.0001 when compared with COPD induced mice.

3.6. Pro-inflammatory cytokines in lung homogenate

CS markedly elevated TNF-α (DC: 88.50 ± 0.76 vs. NC: 19.00 ± 0.37 pg/mg protein; $p < 0.001$) and IL-6 (DC: 72.50 ± 0.43 vs. NC: 14.17 ± 0.31 pg/mg protein; $p < 0.001$) in lung homogenate (Table 8). HEE-HS produced dose-dependent, significant attenuation. At 200 mg/kg, TNF-α was reduced by 49.7% (44.50 ± 0.43 pg/mg) and IL-6 by 50.6% (35.83 ± 0.31 pg/mg) — values approaching the roflumilast group (TNF-α: 40.17 ± 0.48; IL-6: 30.50 ± 0.43 pg/mg; $p < 0.001$ vs. DC for all groups).

Table 8. Pro-inflammatory cytokines in lung homogenate (mean ± SEM, n = 6).

Group	**TNF-α (pg/mg protein)**	**IL-6 (pg/mg protein)**
I – Normal Control	19.00 ± 0.37	14.17 ± 0.31
II – Disease Control	88.50 ± 0.76***	72.50 ± 0.43***
III – Roflumilast 1 mg/kg	40.17 ± 0.48	30.50 ± 0.43
IV – HEE-HS 100 mg/kg	62.50 ± 0.43	51.50 ± 0.43
V – HEE-HS 200 mg/kg	44.50 ± 0.43	35.83 ± 0.31

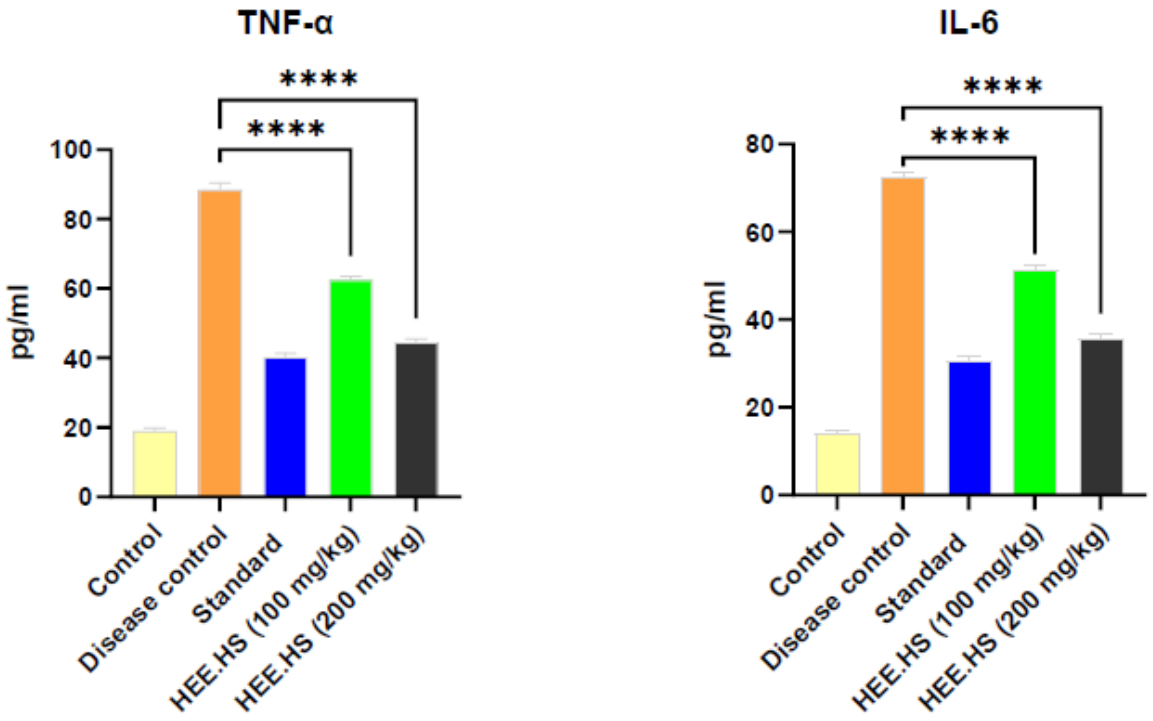

Fig 6. Effect Of Cigarette Smoke Exposure on Pro-Inflammatory Cytokine Levels in Lung Homogenate

All values are expressed as mean ± SEM (n=6). Stastistical comparisions between each treatment and COPD induced mice were carried out by one way ANOVA followed by Turkey multiple comparisions test. ****p < 0.0001 when compared with COPD induced mice.

3.7. Histopathological evaluation

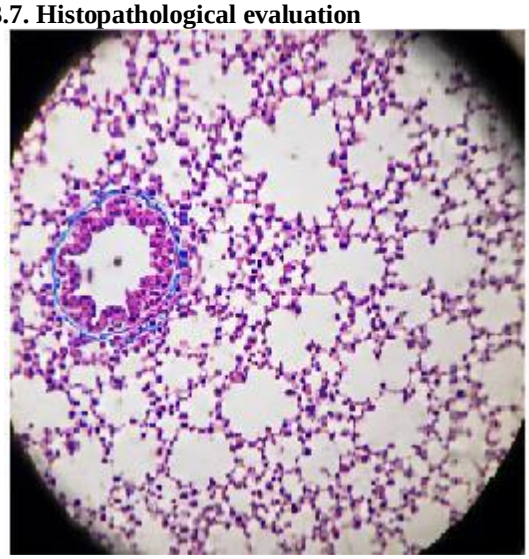

(Fig. 7 A) Displayed intact alveolar architecture, thin delicate septa, no inflammatory infiltrate, and minimal collagen. Roflumilast-treated lungs

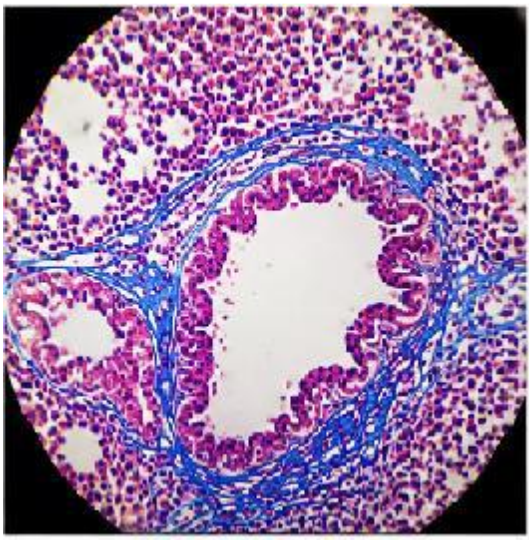

(Fig. 7 B) exhibited:

1. Marked alveolar enlargement with thinned, disrupted septa (emphysema); 2. Dense peribronchial and perivascular inflammatory infiltrate (predominantly neutrophils and macrophages);
3. Goblet cell hyperplasia and bronchial epithelial thickening; and
4. Mucus plugging of bronchioles. Masson's Trichrome staining confirmed extensive peri bronchial collagen deposition indicating advanced airway remodelling. NC sections

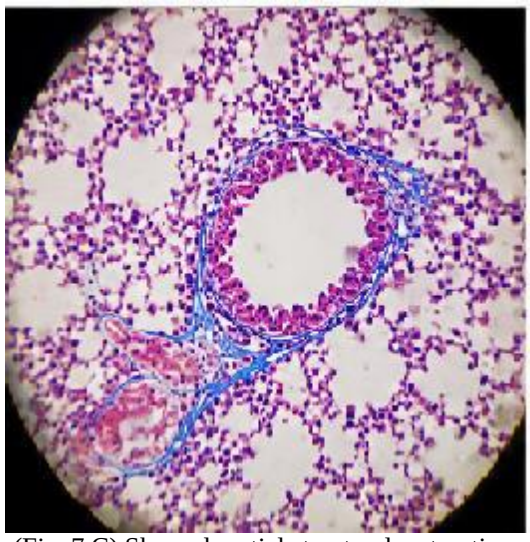

(Fig. 7 C) Showed partial structural restoration, markedly reduced infiltrate, and significantly decreased collagen. HEE-HS at 100 mg/kg

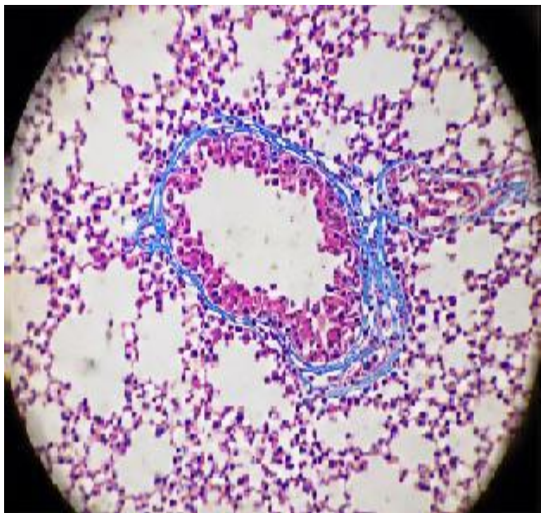

(Fig. 7 D) Produced intermediate improvement with partially restored alveolar structure and reduced but persistent inflammatory infiltrate and partial collagen deposition. Critically, HEE-HS at 200 mg/kg

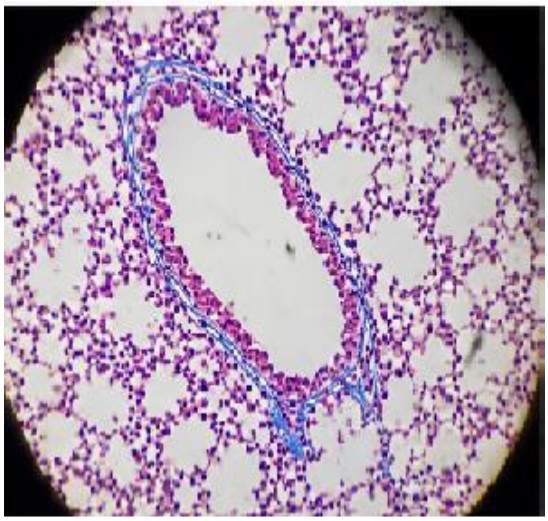

(Fig. 7 E) Produced near-normal alveolar architecture with minimal inflammatory cell infiltration, minimal peri-bronchial collagen deposition, and reduced goblet cell metaplasia — histologically indistinguishable from the roflumilast group.

IV. DISCUSSION

The present investigation is the first systematic multi-parameter preclinical evaluation of HEE HS in a validated cigarette smoke-induced COPD model. The 35-day whole-body CS exposure protocol using research-grade 3R4F cigarettes with precisely characterised TPM, nicotine, and CO yields successfully and reproducibly produced the cardinal features of COPD — progressive body-weight loss, pulmonary hypertrophy, obstructive airflow limitation, BALF neutrophilia, cytokine elevation, and emphysematous histopathology — confirming the validity and reliability of the experimental model.

GC-MS analysis identified 1,8-cineole (28.6%), camphor (15.3%), and β-caryophyllene (12.8%) as the three dominant bioactive constituents of HEE-HS. These compounds collectively provide a mechanistically coherent pharmacological framework for the observed therapeutic benefits. 1,8-Cineole is a well-established inhibitor of NF-κB nuclear translocation and arachidonic acid metabolism, reducing the synthesis of pro-inflammatory prostaglandins and leukotrienes — the precise inflammatory mediators elevated by cigarette smoke exposure. Its ability to directly relax airway smooth muscle and enhance mucociliary clearance further contributes to the bronchodilatory benefit observed through significant $FEV_{0.1}$/FVC restoration. Importantly, 1,8-cineole has also been shown to inhibit TNF-α and IL-6 production via a dual anti-inflammatory mechanism analogous to corticosteroid action, but without the associated adverse effects — directly explaining the greater than 50% cytokine reductions observed at 200 mg/kg.

β-Caryophyllene, as a selective cannabinoid CB2 receptor agonist, suppresses MAPK and NF κB-mediated cytokine production and restores antioxidant enzyme activities — superoxide dismutase and catalase — that are depleted by cigarette smoke-derived reactive oxygen species. Camphor provides complementary mucolytic and mild bronchodilatory activity. The composite multi-constituent pharmacological action of HEE-HS thus offers broader therapeutic coverage than any single-target synthetic agent, addressing inflammation, oxidative stress, and airway obstruction simultaneously.

The BALF analysis provided direct cellular evidence of anti-inflammatory efficacy. Suppression of neutrophil recruitment from 28.33% in disease controls to 13.17% at 200 mg/kg reflects attenuation of chemokine expression — specifically CXCL-1 and CXCL-8 — in alveolar macrophages. These chemokines are the principal drivers of the neutrophil-recruitment cascade responsible for protease and MMP-driven alveolar wall destruction. The simultaneous restoration of macrophage dominance from 58.50% to 78.67% indicates normalisation of the pulmonary immune environment toward homeostasis. The concurrent reductions in TNF-α by 49.7% and IL-6 by 50.6% confirm suppression of the central inflammatory signalling axis of COPD.

The equivalence of HEE-HS 200 mg/kg to roflumilast across all six measured endpoints — $FEV_{0.1}$/FVC ratio, lung weight, lung index, BALF cellular composition, TNF-α, and IL-6 — is clinically meaningful. Roflumilast achieves its anti-inflammatory effects by selectively raising intracellular cyclic AMP in inflammatory cells, thereby suppressing NF-κB-dependent cytokine production. HEE-HS appears to achieve equivalent downstream outcomes through parallel upstream mechanisms — NF

κB/AP-1 blockade, CB2 receptor activation, and arachidonic acid pathway inhibition — yielding statistically indistinguishable results without the gastrointestinal adverse effects commonly associated with roflumilast.

The histopathological near-normalisation of alveolar architecture at 200 mg/kg is a particularly significant finding. No currently approved COPD pharmacotherapy reverses established structural lung damage, yet HEE-HS demonstrated significant structural protection with near-normal alveolar architecture, minimal inflammatory infiltrate, and minimal peri-bronchial collagen deposition that was histologically comparable to roflumilast. This raises the possibility of a disease-modifying potential that warrants dedicated mechanistic investigation, particularly examination of Nrf2-mediated antioxidant pathway activation alongside NF-κB suppression.

The excellent acute safety profile (LD_{50} > 2000 mg/kg per OECD 423) supports a wide therapeutic window suitable for chronic dosing. Delivery by nebulisation directly targets airway inflammation, maximises pulmonary bioavailability of the volatile terpene constituents, and avoids first-pass hepatic metabolism — all advantages over oral administration. Together, the broad-spectrum efficacy, mechanistic coherence, safety profile, and classical Ayurvedic documentation of Shati for Shwasa and Kasa collectively provide the strongest scientific foundation yet for development of HEE HS as a complementary COPD therapeutic.

V. CONCLUSION

The present investigation conclusively demonstrates that HEE-HS at 200 mg/kg, delivered by nebulisation, provides comprehensive, multi-parameter therapeutic efficacy in cigarette smoke induced COPD statistically equivalent to the clinical standard roflumilast.

The key conclusions are:

- COPD model: CS exposure for 35 days successfully and reproducibly induced COPD-like airflow obstruction, pulmonary neutrophilia, cytokine elevation, and emphysematous histopathology. • HEE-HS characterisation: extract yield 2.38% w/w; dominant GC-MS constituents: 1,8-cineole (28.6%), camphor (15.3%), β-caryophyllene (12.8%); confirmed alkaloids, saponins, flavonoids, tannins, glycosides, and reducing sugars.
- Acute oral toxicity studies confirmed the safety of Hydroethanolic extract of H. spicatum, with LD_{50} > 2000 mg/kg, supporting its favourable safety profile for chronic administration. • Pulmonary function: $FEV_{0.1}$/FVC restored from 54.3% (DC) to 78.0% at 200 mg/kg (+43.6%) — equivalent to roflumilast (78.1%).
- BALF: total cell count reduced ~2.6-fold; neutrophil % from 28.33% to 13.17%; macrophage dominance restored to 78.67% — all comparable to roflumilast.
- Cytokines: TNF-α reduced by 49.7% (44.50 pg/mg) and IL-6 by 50.6% (35.83 pg/mg) — approaching roflumilast levels.
- Histopathological evaluation confirmed marked reduction in emphysematous alveolar changes, inflammatory infiltration, goblet cell metaplasia, and airway collagen deposition in treated groups.

These findings provide the first robust, multi-parameter preclinical evidence validating the Ayurvedic use of H. spicatum in respiratory conditions and strongly advocate mechanistic pathway delineation (Nrf2/NF-κB), pharmacokinetic profiling of the nebulised formulation, and Phase I/II clinical translation.

REFERENCES

[1]. Vestbo J, Hurd SS, Agustí AG, Jones PW, Vogelmeier C, Anzueto A, et al. Global strategy for the diagnosis, management, and prevention of chronic obstructive pulmonary disease: GOLD executive summary. Am J Respir Crit Care Med. 2013;187(4):347–365. doi:10.1164/rccm.201204-0596PP

[2]. Global Initiative for Chronic Obstructive Lung Disease (GOLD). Global strategy for the diagnosis, management, and prevention of COPD: 2024 Report [Internet]. Available from: https://goldcopd.org

[3]. Rabe KF, Watz H. Chronic obstructive pulmonary disease. Lancet. 2017;389(10082):1931–1940. doi:10.1016/S0140-6736(17)31222-9

[4]. World Health Organization. COPD fact sheet [Internet]. Geneva: WHO; 2023. Available from: https://www.who.int/news-room/fact-sheets/detail/chronic-obstructive-pulmonary-disease- (copd)

[5]. Inocencio TJ, Sterling KL, Sayiner S, Minshall ME, Kaye L, Hatipoğlu U.

Budget impact analysis of a digital monitoring platform for COPD. Cost Eff Resour Alloc. 2023;21:36. doi:10.1186/s12962-023-00443-x

[6]. Jindal SK, Aggarwal AN, Chaudhry K, Chhabra SK, D'Souza GA, Gupta D, et al. A multicentric study on epidemiology of COPD and its relationship with tobacco smoking. Indian J Chest Dis Allied Sci. 2006;48(1):23–29.

[7]. Salvi SS, Barnes PJ. Chronic obstructive pulmonary disease in non-smokers. Lancet. 2009;374(9691):733–743. doi:10.1016/S0140-6736(09)61303-9

[8]. Adair-Kirk TL, Atkinson JJ, Griffin GL, Watson MA, Kelley DG, DeMello D, et al. Distal airways in mice exposed to cigarette smoke: Nrf2-regulated genes are increased in Clara cells. Am J Respir Cell Mol Biol. 2008;39:400–411. doi:10.1165/rcmb.2007-0295OC

[9]. MacNee W. Oxidative stress and lung inflammation in airways disease. Eur J Pharmacol. 2001;429(1–3):195–207. doi:10.1016/S0014-2999(01)01320-6

[10]. Rahman I, Adcock IM. Oxidative stress and redox regulation of lung inflammation in COPD. Eur Respir J. 2006;28(1):219–242. doi:10.1183/09031936.06.00053805

[11]. Hogg JC, Timens W. The pathology of chronic obstructive pulmonary disease. Annu Rev Pathol. 2009;4:435–459. doi:10.1146/annurev.pathol.4.110807.092145

[12]. Shapiro SD, Ingenito EP. The pathogenesis of COPD: advances in the past 100 years. Am J Respir Cell Mol Biol. 2005;32(5):367–372. doi:10.1165/rcmb.F296

[13]. Saetta M, Di Stefano A, Turato G, Facchini FM, Corbino L, Mapp CE, et al. CD8+ T-lymphocytes in peripheral airways of smokers with COPD. Am J Respir Crit Care Med. 1998;157(3 Pt 1):822–826. doi:10.1164/ajrccm.157.3.9709027

[14]. Stoller JK, Aboussouan LS. A review of alpha1-antitrypsin deficiency. Am J Respir Crit Care Med. 2012;185(3):246–259. doi:10.1164/rccm.201108-1428CI

[15]. Fahy JV, Dickey BF. Airway mucus function and dysfunction. N Engl J Med. 2010;363(23):2233–2247. doi:10.1056/NEJMra0910061

[16]. Rogers DF. Physiology of airway mucus secretion and pathophysiology of hypersecretion. Respir Care. 2007;52(9):1134–1146.

[17]. Martinez FJ, Rabe KF, Sethi S, Pizzichini E, McIvor A, Anzueto A, et al. Effect of roflumilast and ICS/LABA on COPD exacerbations (RE2SPOND). Am J Respir Crit Care Med. 2016;194(5):559–567. doi:10.1164/rccm.201607-1349OC

[18]. Calverley PMA, Rabe KF, Goehring UM, Kristiansen S, Fabbri LM, Martinez FJ. Roflumilast in symptomatic COPD: two randomised clinical trials. Lancet. 2009;374(9691):685–694. doi:10.1016/S0140-6736(09)61255-1

[19]. Hankey A. CAM modalities can stimulate advances in theoretical biology. Evid Based Complement Alternat Med. 2005;2(1):5–12. doi:10.1093/ecam/neh065

[20]. Debnath PK, Chattopadhyay J, Mitra A, Adhikari A, Alam MS, Bandyopadhyay SK, et al. Adjunct therapy of Ayurvedic medicine with anti-tubercular drugs. J Ayurveda Integr Med. 2012;3(3):141–149. doi:10.4103/0975-9476.100180

[21]. Kumari I, Maheshwari R, Jyoti S. Hedychium spicatum: a review of its traditional uses, phytochemistry and pharmacological activities. J Pharm Phytochem. 2021;10(1):58–66.

[22]. Joshi S, Chanotiya CS, Agarwal G, Agrawa O, Khare A, Bhatt AK. Terpenoid compositions and antioxidant and antimicrobial properties of the rhizome essential oils of different Hedychium species. Chem Biodivers. 2008;5(2):299–309. doi:10.1002/cbdv.200890026

[23]. Worth H, Schacher C, Dethlefsen U. Concomitant therapy with cineole (eucalyptole) reduces exacerbations in COPD: a placebo-controlled double-blind trial. Respir Res. 2009;10:69. doi:10.1186/1465-9921-10-69

[24]. Juergens UR, Engelen T, Racke K, Stober M, Gillissen A, Vetter H. Inhibitory activity of 1,8- cineol (eucalyptol) on cytokine production in cultured human lymphocytes and monocytes. Pulm Pharmacol Ther. 2004;17(5):281–287. doi:10.1016/j.pupt.2004.06.002

[25]. O'Callaghan C, Barry PW. The science of nebulised drug delivery. Thorax.

1997;52(Suppl 2):S31– 44. doi:10.1136/thx.52.2008.S31

[26]. Dolovich MB, Dhand R. Aerosol drug delivery: developments in device design and clinical use. Lancet. 2011;377(9770):1032–1045. doi:10.1016/S0140-6736(10)60926-9

[27]. Adorjan B, Buchbauer G. Biological properties of essential oils: an updated review. Flavour Fragr J. 2010;25(6):407–426. doi:10.1002/ffj.2024

[28]. Ghildiyal S, Gautam MK, Joshi VK, Goel RK. Pharmacological evaluation of extracts of Hedychium spicatum (Ham. ex Smith) rhizome. Indian J Exp Biol. 2012;50(6):408–413.